Journal of Bioenergetics and Biomembranes (2019) 51:341–354
https://doi.org/10.1007/s10863-019-09807-6

Increased reactive oxygen species production and maintenance of membrane potential in VDAC-less *Neurospora crassa* mitochondria

Sabbir R. Shuvo[1,2] · Lilian M. Wiens[3] · Saravananaidu Subramaniam[1] · Jason R. Treberg[3,4] · Deborah A. Court[1]

Received: 19 September 2018 / Accepted: 18 July 2019 / Published online: 7 August 2019

Abstract

The highly abundant voltage-dependent anion-selective channel (VDAC) allows transit of metabolites across the mitochondrial outer membrane. Previous studies in *Neurospora crassa* showed that the LoPo strain, expressing 50% of normal VDAC levels, is indistinguishable from wild-type (WT). In contrast, the absence of VDAC (ΔPor-1), or the expression of an N-terminally truncated variant VDAC (ΔN2-12porin), is associated with deficiencies in cytochromes *b* and aa_3 of complexes III and IV and concomitantly increased alternative oxidase (AOX) activity. These observations led us to investigate complex I and complex II activities in these strains, and to explore their mitochondrial bioenergetics. The current study reveals that the total NADH dehydrogenase activity is similar in mitochondria from WT, LoPo, ΔPor-1 and ΔN2-12porin strains; however, in ΔPor-1 most of this activity is the product of rotenone-insensitive alternative NADH dehydrogenases. Unexpectedly, LoPo mitochondria have increased complex II activity. In all mitochondrial types analyzed, oxygen consumption is higher in the presence of the complex II substrate succinate, than with the NADH-linked (complex I) substrates glutamate and malate. When driven by a combination of complex I and II substrates, membrane potentials (Δψ) and oxygen consumption rates (OCR) under non-phosphorylating conditions are similar in all mitochondria. However, as expected, the induction of state 3 (phosphorylating) conditions in ΔPor-1 mitochondria is associated with smaller but significant increases in OCR and smaller decreases in Δψ than those seen in wild-type mitochondria. High ROS production, particularly in the presence of rotenone, was observed under non-phosphorylating conditions in the ΔPor-1 mitochondria. Thus, the absence of VDAC is associated with increased ROS production, in spite of AOX activity and wild-type OCR in ΔPor-1 mitochondria.

Keywords VDAC · Mitochondrial porin · *Neurospora crassa* · Alternative oxidase · Membrane potential · Reactive oxygen species

Introduction

Voltage-dependent anion-selective channels (VDAC), also known as mitochondrial porins, provide the primary transport mechanism across the mitochondrial outer membrane (MOM) for ADP, ATP and small organic anions that include respiratory substrates. They are proposed to regulate calcium, metabolite and ATP/ADP flow through the MOM, from the intermembrane space to the cytosol and vice-versa (Fig. 1; see (Shoshan-Barmatz and De 2017)). VDAC folds into a 19 β-stranded barrel with an extra-membranous N-terminal α-helix that resides in the barrel lumen in the folded state subjected to structural analysis (Bayrhuber et al. 2008; Hiller et al. 2008; Ujwal et al. 2008). The helix is proposed to re-orient and become exposed to the cytosol in the partially closed states

Electronic supplementary material The online version of this article (https://doi.org/10.1007/s10863-019-09807-6) contains supplementary material, which is available to authorized users.

✉ Deborah A. Court
Deborah.Court@umanitoba.ca

[1] Department of Microbiology, University of Manitoba, Winnipeg, MB R3T 2N2, Canada

[2] Present address: Department of Biochemistry and Microbiology, North South University Dhaka, Dhaka, Bangladesh

[3] Department of Biological Sciences, University of Manitoba, Winnipeg, MB R3T 2N2, Canada

[4] Department of Food and Human Nutritional Sciences, University of Manitoba, Winnipeg, MB R3T 2N2, Canada

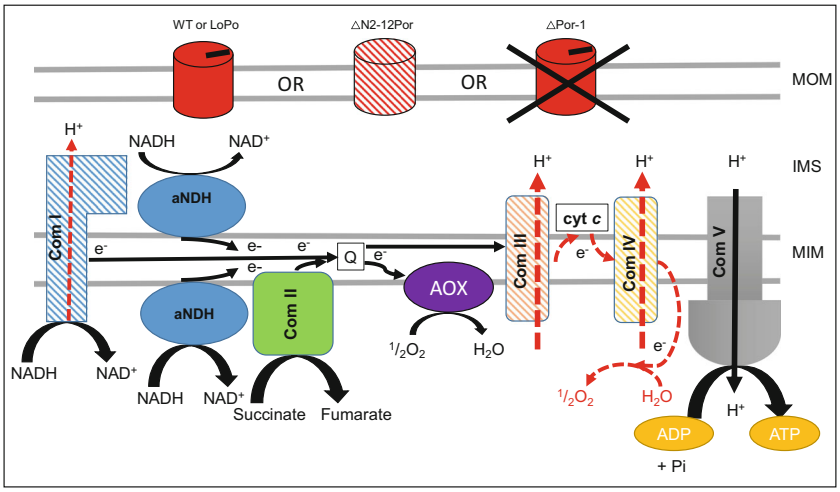

Fig. 1 Electron transport and oxidative phosphorylation in wild-type and variant *Neurospora crassa* mitochondria. In WT mitochondria CoQ (Q) shuttles electrons from complex I (Com I), complex II (Com II) and the four alternative NAD(P)H dehydrogenases (aNDH), to complex III (Com III). Electrons from Com III are carried by cytochrome *c* (cyt *c*) to Complex IV (Com IV). ATP synthase (Com V) uses the resulting proton gradient for ATP synthesis. Note that complexes I, III and IV exist in supercomplexes with compositions of ComI-ComIV, ComI-ComIII, ComI-ComIII-ComIV and that complexes I and V form homodimers in *N. crassa* (Marques et al. 2007). Three variant strains were used: LoPo, expressing 40–50% of WT levels of VDAC, ΔPor-1, lacking VDAC, and ΔN2-12Por, expressing an N-terminally truncated VDAC at about 10% of WT levels. With the exception of an increased level of Com II activity, the ETC of LoPo resembles that of WT (not shown). In ΔPor-1 and ΔN2-12Por mitochondria, the cytochromes associated with complexes III and IV are reduced (hatched symbols), cytochrome *c* is present in higher levels, and electrons are shuttled from the Q-pool through alternative oxidase (AOX). Additionally, in ΔPor-1, complex I levels are decreased and aNDH activity is higher than in WT. The predicted reductions in proton pumping are indicated by dotted lines. VDAC is shown as a red cylinder with a black stick that indicates the N-terminus; the crossed out symbol represents the lack of VDAC in ΔPor-1 and the hatched cylinder lacking the stick indicates the truncation in ΔN2-12Por and the lower levels of this protein. *N. crassa* has four alternative NAD(P)H dehydrogenases (aNDH), one on the matrix side and three in the MIM. For clarity, only one of each group is shown. MOM, mitochondrial outer membrane; MIM, mitochondrial inner membrane; IMS, inter membrane space

associated with gating (Geula et al. 2012, Tomasello et al. 2013). Partial truncation of the N-terminus of VDAC from *Neurospora crassa* generates a protein that forms gated, but unstable, channels in artificial membranes (Popp et al. 1996), and in vivo, this truncation is associated with a reduced level of VDAC and defects in the electron transport chain (Shuvo et al. 2017). While VDAC can modulate multiple cellular functions via interactions with other proteins, the connections between VDAC and mitochondrial bioenergetics have yet to be examined in detail.

N. crassa is an excellent candidate for studying the effect that the absence of VDAC has on mitochondrial bioenergetics and reactive oxygen species (ROS) production. It is an obligate aerobe and has canonical respiratory chain complexes I through V, some of which exist in supercomplexes ((Marques et al. 2007) and see legend to Fig. 1). In addition, it expresses several alternative non-proton-pumping NAD(P)H dehydrogenases (Fig. 1; (Carneiro et al. 2012)). Isolation of mitochondria from *N. crassa* is straightforward and therefore, this fungus has been used extensively for the study of mitochondrial biology (see reviews by (Nargang and Rapaport 2007) and (Videira and Duarte 2002)) and of VDAC function, starting with the initial experiments by (Colombini 1979). In addition, *N. crassa* expresses a single VDAC isoform, in contrast to mammalian systems in which an understanding of the effects of a knockout of VDAC is complicated by the presence of three VDAC isoforms, one of which is required for embryonic development (reviewed in (Young et al. 2007)).

In *N. crassa,* while VDAC is not essential, a strain (ΔPor-1) lacking this channel has severe mitochondrial abnormalities and high alternative oxidase (AOX) activity (Table 1; Summers et al. 2012). AOX receives electrons from ubiquinol (reduced CoQ) and thus bypasses complex III and IV to donate electrons to terminal oxygen (Fig. 1). Hence, energy from the electrons that pass through AOX contributes less to the formation of the proton motive force across the inner membrane (Møller 2001; Tanton et al. 2003). AOX has been proposed to reduce ROS production by allowing alternative electron flow in the inner membrane, thereby preventing build-up of a highly reduced pool of CoQ (Q-pool) (Maxwell et al. 1999).

There is limited information on mitochondrial ROS production in *N. crassa*, in particular from VDAC-impaired strains. During mitochondrial energy transformation processes, electrons can leak and partially reduce oxygen to produce reactive oxygen species. In broad terms, ROS refers to oxygen molecules that are chemically reactive, without the need for a catalyst (Munro and Treberg 2017). Examples of ROS are singlet oxygen, hydrogen peroxide, hydroxyl radical and superoxide anion. In mitochondria, ROS are produced from complex I, II and III of the ETC (Fig. 2) and enzymes of the tricarboxylic acid (TCA) cycle (reviewed in (Mailloux 2015)). Most of the mitochondrial ROS producing sites catalyze

Table 1 Summary of *N. crassa* strains and ETC data

Strain name	Genotype/Comments	Respiration insensitive to cyanide (%) [a]	Cytochrome aa_3 and b levels (Complexes III and IV)	NADH dehydrogenase activities [b]	Complex II activity [c]
FGSC 9718[d] (wild-type; WT)	*Δmus-51::bar*$^+$ *mat a* (Colot et al. 2006)	< 5% (Summers et al. 2012)	WT (Summers et al. 2012), (Shuvo et al. 2017)	tNDH: 100% aNDH: 100% complex I: 100%	100%
LoPo	*hph*$^+$, *Δmus51::bar* + *mat α, TOM40 promoter::por* transformant of FGSC 9718 (Shuvo et al. 2017)	8% (Shuvo et al. 2017)	Similar to WT (Shuvo et al. 2017)	tNDH: 103% aNDH: 101% complex I: 104%	153%*
ΔPor-1	*Δpor::hph*$^+$ *Δmus51::bar*$^+$ *mat a* transformant of FGSC 9718 (Summers et al. 2012)	95% (Summers et al. 2012)	Reduced (Summers et al. 2012)	tNDH: 88% aNDH:148% complex I: 30%*	84%
ΔN2-12porin	*hph*$^+$, *porΔ2–12, Δmus51::bar*$^+$ *mat a* transformant of FGSC 9718 (Shuvo et al. 2017)	80% (Shuvo et al. 2017)	Reduced (Shuvo et al. 2017)	tNDH: 96% aNDH:134% complex I: 60%*	84%

[a] Measured as percentage of oxygen consumption that occurs in the presence of cyanide; mediated by alternative oxidase

[b] Data from Fig. 4a; relative to WT; tNDH, total NDH actvity; aNDH, alternative NDH activity

[c] Data from Fig. 4b; relative to WT

[d] Strain FGSC 9718 was obtained from the Fungal Genetics Stock Center (McCluskey et al. 2010)

[*] Different than WT (students' t-test <0.5)

conversion of monovalent oxygen to superoxide, which is rapidly dismuted to hydrogen peroxide either spontaneously or by superoxide dismutase (SOD) activity in the matrix or the intermembrane space; in addition, some sites can generate hydrogen peroxide from divalent reduction of oxygen (Brand 2010).

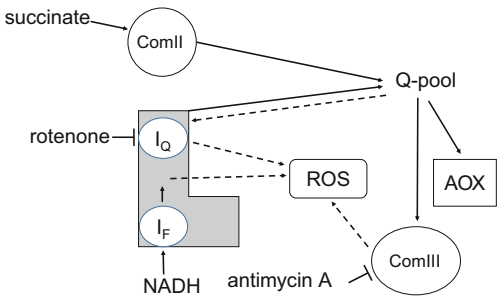

Fig. 2 ROS production sites in the ETC. Rotenone and antimycin A induce ROS production by interactions with complex I (grey L-shape) and complex III (ComIII), respectively. The two ROS producing sites in complex I are associated with the flavin mononucleotide (I_F) and ubiquinone (I_Q); rotenone blocks the I_Q site, increasing ROS production by NADH-linked substrates. Reverse flow from succinate to complex I, via complex II (ComII) can occur, but is greatly decreased in the presence of glutamate, malate and NADH-linked substrates, likely due to inhibition of ComII (discussed in Muller et al. 2008). Sites of inhibitor activity are indicated by blunt ended lines, and solid and dashed arrows indicate electron flow in the absence or presence of inhibitors, respectively. In the presence of inhibitors, the CoQ(red)/CoQ(ox) ratio is high. Antimycin A treatment blocks interactions between the Q-pool and CIII at Qi, leading to ROS generation. Alternative oxidase can decrease the CoQ(red)/CoQ(ox) ratio, thereby limiting ROS production in cells where oxidation of the Q-pool is blocked by inhibitors or defects in the ETC. Other mitochondrial ROS-producing sites (Brand 2010; Mailloux 2015) are not shown. Note that ROS can also be produced directly from complex II (Quinlan et al. 2012)

In this study, the characterization of the ETC in a group of VDAC knockdown (LoPo), knockout (ΔPor-1) and VDAC variant (ΔN2-12porin) strains was completed with measurements of NADH dehydrogenase and succinate dehydrogenase activities. The following hypotheses were addressed i) in order to maintain membrane potential, mitochondria from strains with ETC defects and expressing AOX will consume oxygen at higher rates, due to the fact these defects may lead to higher ratios of oxygen consumed to protons pumped ii) that AOX activity will be sufficient to drive electron flux away from complexes I and II, thus maintaining reducing potential (lower ratios of reduced (CoQ(red)) to oxidized CoQ (CoQ(ox))) and thereby maintaining low levels of ROS in the presence of abnormal ETC. To these ends, respiration rates, relative measurements of membrane potential, and ROS production were examined.

Materials and methods

Chemicals

All the chemicals were purchased from Thermo Fisher Scientific (Mississauga, ON, Canada), Sigma-Aldrich Canada (Oakville, ON, Canada) or BioShop Canada (Burlington, ON, Canada).

Strains and growth conditions

N. crassa strains used in this study are listed in Table 1. Note that VDAC from *N. crassa* is also referred to as mitochondrial porin, and the porin designation is incorporated into the names

of the VDAC variants (Popp et al. 1996) and strains (Summers et al. 2012). Growth and handling of *N. crassa* strains were performed following the procedures described in (Davis and de Serres 1970) at 30 °C. Mitochondria were isolated following the modification of the protocol described in (Harkness et al. 1994). In brief, mycelia were harvested by filtration from 14 to 16-h (wild-type and LoPo) or 20-h (ΔN2-12porin) or 36-h ΔPor-1 liquid cultures. The mycelial mats were ground with sand in SEM buffer (220 mM sucrose, 1 mM EDTA, 10 mM MOPS [morpholinepropanesulfonic acid], pH 7.2]. Sand and unbroken hyphae were removed by two rounds of centrifugation for 5 min each at 3000×g and mitochondria were collected by centrifugation of the resulting supernatant for 12 min at 17000×g. All steps were carried out on ice or at 4 °C. Further purification on flotation gradients was not used, as it can lead to disruption of the MOM (see (Ferens et al. 2017) for discussion).

Evaluation of mitochondrial outer membrane integrity

Mitochondrial outer membrane integrity was evaluated based on the change in oxygen consumption in response to addition of exogenous cytochrome *c*. Briefly, 100 μg of mitochondrial protein was added to 2 ml of air-equilibrated SR buffer (modified from (Court et al. 1996); 50 mM KH_2PO_4, 5 mM $MgCl_2$, 10 mM MOPS, 250 mM sucrose, 0.3% fatty acid free BSA, pH 7.2) at 30 °C in an Oxygraph-2 k (Oroboros Instruments, Innsbruck, Austria). After stabilization of the signal, succinate and rotenone (the latter dissolved in DMSO) were added to final concentrations (fc) of 5 mM and 1 μM, respectively. The mitochondria reached a stable respiration rate under these non-phosphorylating conditions (state 2). Subsequent addition of 1 mM ADP initiated phosphorylating respiration (state 3). Lastly, 8 μM (fc) of cytochrome *c* was added to determine the oxygen consumption rate to evaluate MOM integrity. The degree of broken MOM was evaluated by dividing the oxygen consumption rate in the presence of ADP and exogenous cytochrome *c* by the oxygen consumption rate in the presence of ADP alone (×100) (Banh et al. 2015). It is related to the amount of exogenous cytochrome *c* that can enter the intermembrane space to increase electron flux to complex IV, thereby, increasing the respiration rate (Supplementary Fig. 1). The validity of this ratio as a measure of intactness was confirmed by a parallel set of experiments, for each strain, in which two samples of each mitochondrial preparation were mixed in the respirometer under the same buffer conditions as for the cytochrome *c*-based assay. The membrane integrity test described above was carried out in one chamber, and from the other samples were removed for western blotting (see Supplementary Fig. 1B for details). In brief, samples (125 μg of mitochondrial protein in 0.5 ml SR buffer) were either untreated, or digested with proteinase K (final concentration 10 μg/ml) on ice for 15 min. Protease digestion was stopped by the addition of PMSF (4 mM final concentration) and mitochondria were collected by centrifugation, and suspended in 50 μl of 4x SDS loading buffer (20 mM Tris-Cl pH 8.0, 40% glycerol, 4% SDS, 0.004% (*w*/*v*) bromophenol blue, 20 mM β-mercaptoethanol). Proteins were separated by SDS-PAGE, transferred to nitrocellulose and probed with antibodies against Tom70, cytochrome c heme lyase (CCHL) and the mitochondrial-processing peptidase (MPP). Tom70 resides in the MOM and is susceptible to externally added protease while CCHL is localized to the intermembrane space and will be protected from externally added protease in intact mitochondria (see (Schlossmann et al. 1994)). MPP is a matrix protein (Schneider et al. 1990), and will be protease-protected unless the inner membrane is ruptured. It was used as a loading control.

Complex I and complex II activity

NADH dehydrogenase (NDH) activity was measured using n-dodecyl β-D-maltoside (DDM) solubilized mitochondria. 300 μg of mitochondrial protein were dissolved in 100 μl of 1% (*w*/*v*) DDM in 20 mM Tris-Cl pH 7.4, 0.1 mM EDTA, 50 mM NaCl, as described in (Ferens et al. 2017). Samples were incubated on ice for 20 min followed by centrifugation at 15000 rpm in a microfuge for 15 min at 4 °C. NDH activity of 15–25 μl of the resulting suspension was assayed in 1 ml of NDH assay buffer (0.25 M sucrose, 50 mM Tris-Cl pH 8.0, 0.2 mM EDTA, 0.3% (w/v) fatty-acid free BSA (Marques et al. 2005)). Reactions were started by the addition of NADH (fc 100 μM). The reactions were allowed to proceed for 2 min to establish full activity, and then either 1 μl of 10 mM rotenone in DMSO, or 1 μl DMSO (solvent control) was added. The reactions were allowed to continue for six minutes. Rates of rotenone-sensitive and rotenone-insensitive oxidation of NADH were calculated from the decrease in OD at 340 nm, and the corresponding change in NADH concentration was determined using the molar extinction coefficient of 6.22×10^3 M^{-1}. cm^{-1}. Rates were normalized to mg of mitochondrial extract added to the reaction.

Mitochondrial complex II activity was measured based on the protocol described in (Frazier and Thorburn 2012). Briefly, 50 μg of previously frozen mitochondrial protein was suspended in 1 ml of complex II buffer (50 mM KH_2PO_4, 10 mM succinate, 1 mM KCN, 2.5 μM rotenone, 10 μM antimycin A, pH 7.4) and incubated at 23 °C to activate complex II. The reaction was started by adding coenzyme Q_1 (CoQ_1) from a stock solution in DMSO (fc 20 μM). Reduction of CoQ via complex II activity was measured by decreased absorbance at 280 nm. The activity (nmol min^{-1}) was calculated using the extinction coefficient for reduced CoQ_1 of 12 mM^{-1} cm^{-1} and then normalized to the amount of protein (nmol min^{-1} mg^{-1}).

Simultaneous measurement of respiration rate and membrane potential

Combined respirometry and spectrofluorometry were conducted using 100 μg of mitochondrial protein in 2 ml of SR buffer containing 2.5 μM tetramethylrhodamine methyl ester (TMRM) at 30 °C in an Oxygraph-2 k. In state 2 respiration, the oxygen consumption rate in the presence and absence of TMRM was measured in reaction media containing 5 mM glutamate, 5 mM succinate and 5 mM malate (GMS), supporting electron entry into the electron transport system at complex I and complex II (Hoffman and Brookes 2009). Glutamate and malate (GM), and succinate (S) alone, were also utilized at the same final concentrations. To initiate state 3 respiration, ADP was added to 800 μM, followed by oligomycin (fc 1 μM) to measure the oligomycin-induced, non-phosphorylating respiration rate (state 4o).

Accumulation of the lipophilic cationic fluorescent dye TMRM was used to estimate membrane potential (ΔΨ). Quenching TMRM fluorescence in response to its migration into the organelle is proportional to the degree of mitochondrial energization (see (Chowdhury et al. 2016)). Here we assume that TMRM has comparable non-specific binding to all mitochondrial types and that the matrix volumes per mg of mitochondria protein across strains are similar. Reaction conditions for measuring ΔΨ were as described for determining respiration rate, except that 10 μM CCCP (Carbonyl cyanide 3-chlorophenylhydrazone) was introduced to depolarize the mitochondria at the end of the experiment. Relative TMRM fluorescence quenching was used to assess relative ΔΨ in different states of respiration (see Fig. 3).

To the best of our knowledge this is the first time TMRM was utilized to study the *N. crassa* mitochondrial ΔΨ and it was necessary to confirm that TMRM did not influence mitochondrial respiration. A moderate, but statistically significant effect of TMRM on respiration was seen only in WT (Supplementary Fig. 2). In the presence of TMRM, WT state 2 respiration was about 20–25% lower than that in the absence of TMRM; a similar reduction was noted for mouse cortical cells in TMRM and was predicted to be due to effects on ATP synthase activity (Chowdhury et al. 2016). However, in the presence and absence of TMRM, the RCRo was unchanged when evaluated using an oligomycin-induced non-phosphorylating state of respiration (state 4o; Supplementary Table 1). Thus, TMRM at 2.5 μM does not interfere significantly with coupling and is a suitable tool for comparison of ΔΨ in *N. crassa* mitochondria.

Mitochondrial H_2O_2 efflux measurements

Mitochondrial ROS production was measured as H_2O_2 efflux using the protocol described in (Banh and Treberg 2013). Briefly, 200 μg of mitochondrial protein was suspended in

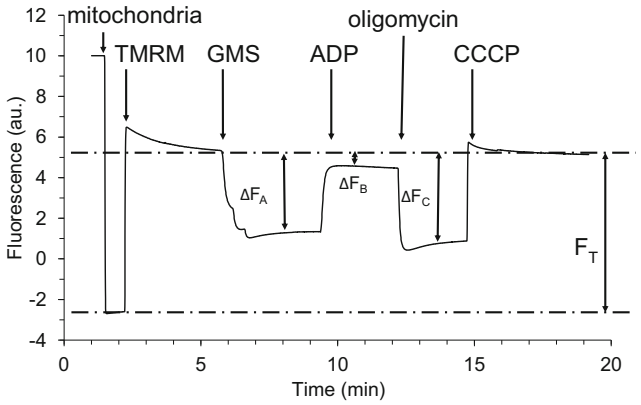

Fig. 3 Measurement of relative ΔΨ in WT mitochondria by quenching of TMRM fluorescence. A representative trace using WT mitochondria is shown; additions are indicated by the arrows in the top part of the figure. In the presence of GMS (state 2 respiration), mitochondria were energized and fluorescence was quenched (ΔF_A) as TMRM entered the mitochondria. Subsequently, ADP was used to depolarize the mitochondria (state 3 respiration) and dequenching was observed (ΔF_B). Next, oligomycin was used to inhibit the ATP synthesis from complex V (state 4o respiration), and fluorescence was quenched (ΔF_C). Finally, to obtain the fully uncoupled stage, CCCP was added. The difference between deenergized and background fluorescence (F_T) was determined as the difference between the lowest fluorescence (upper dashed line), which was observed in the closed chamber with mitochondria and buffer alone, and the highest stable fluorescence, in uncoupled mitochondria (+CCCP, lower dashed line)

2 ml of SR buffer. 25 $IUml^{-1}$ superoxide dismutase (SOD, to minimize autoxidation of Amplex Ultrared and convert any extramitochondrially directed superoxide to H_2O_2), 5 $IUml^{-1}$ horseradish peroxidase (which carries out the oxidation of Amplex Ultrared in the presence of H_2O_2), and 50 μM Amplex Ultrared were used in the reaction buffer. The fluorescence was measured at 30 °C with constant stirring, at an excitation wavelength of 550 nm and an emission wavelength of 590 nm in an Agilent Eclipse spectrofluorometer. After monitoring for a 5 min preincubation phase, GMS was added and the reaction was allowed to continue for at least 5 min to determine the rate of H_2O_2 efflux. Calibration curves were constructed by using at least 4 stepwise additions of 0.2 nmole of H_2O_2 to identical cuvettes with mitochondria in the presence or absence of respiratory substrates. The rate of increase in fluorescence was converted to nmole of H_2O_2 min^{-1} mg^{-1} $protein^{-1}$ based on this curve. The fluorescence values were slightly lower in the absence of respiratory substrates; for example, for ΔPor-1, the values were 167 and 150 arbitrary units per nmole of H_2O_2 in the presence and absence of substrate. To evaluate the possible role of specific enzyme complexes in ROS production, 0.5 μM rotenone and 10 μM antimycin A were used separately as inhibitors for complex I and complex III, respectively. Rotenone binds to the Q-binding site of complex I (I_Q) and antimycin A blocks the transfer of electrons in the Q_i site of complex III (Liu et al. 2002; Fig. 2).

Statistical analysis

The results are presented as mean ± SD (standard deviation). Given the multiple variables (VDAC, AOX levels and ETC) among the strains analyzed (see below), pairwise comparisons between the WT and each variant were performed for complex II activity, membrane potential, ROS production and RCRo. These data were analyzed using Student's t test; $p < 0.05$ was considered significant. For analyzing the effect of TMRM on the overall RCRo data, ANOVA was used, followed by the PAIRWISE Tukey test.

Results

N. crassa ETC complexes and VDAC

In the wild-type (WT) *N. crassa* strain, the ETC is composed of the canonical complexes I through V, and, in addition, this fungus expresses four rotenone-insensitive, non-proton pumping alternative NAD(P)H dehydrogenases (aNDH), one of which faces the matrix side of the mitochondrial inner membrane (Fig. 1) (Gonçalves and Videira 2015). To provide a baseline for comparisons with other strains, the total NADH dehydrogenase (tNDH) activity and complex II activity were determined for WT (Fig. 4). tNDH activity was assessed in solution in the presence and absence of the complex I inhibitor, rotenone (Fig. 4a), to distinguish the aNDH activity from the total activity. In WT, about 50% of the NDH activity is rotenone-sensitive and represents complex I activity.

The high abundance of VDAC (Schein et al. 1976) suggests that many pores are needed for its many normal functions. However, a strain (LoPo) expressing 40–50% of VDAC has cytochrome spectra and growth characteristics indistinguishable from WT (Shuvo et al. 2017). Therefore, it was hypothesized that in LoPo, complex I and II activity would be similar to WT. In isolated LoPo mitochondria, tNDH and aNDH activities were indistinguishable from WT (Fig. 4a), but the activity of complex II was increased by about 50% compared to WT (Fig. 4b), indicating an unexpected consequence of reduction of VDAC levels.

In contrast to WT and LoPo, the VDAC knockout strain, ΔPor-1 displays deficiencies in the cytochromes residing in complex III (cytochrome *b*, about 40% of WT) and complex IV (cytochrome aa_3, 25% of WT) and an increase (150% of WT) in levels of cytochrome *c* (Summers et al. 2012). Unlike WT, the ΔPor-1 strain expresses alternative oxidase (AOX; Table 1), which can bypass complex III and complex IV to donate electrons to the terminal oxygen (Fig. 1). Proteomic analyses of ΔPor-1 mitochondria indicated low levels of some of the subunits of complex I ((Summers et al. 2012) (Ferens et al. 2017)), suggesting that complex I activity is low in this strain. This hypothesis is supported by the reduced levels of rotenone-sensitive NDH activity (~20% of WT, Fig. 4a). Nonetheless, the tNDH activity per mg of mitochondrial extract is similar to that of WT, presumably to ensure sufficient NAD^+. The increase in aNDH activity can be attributed to the

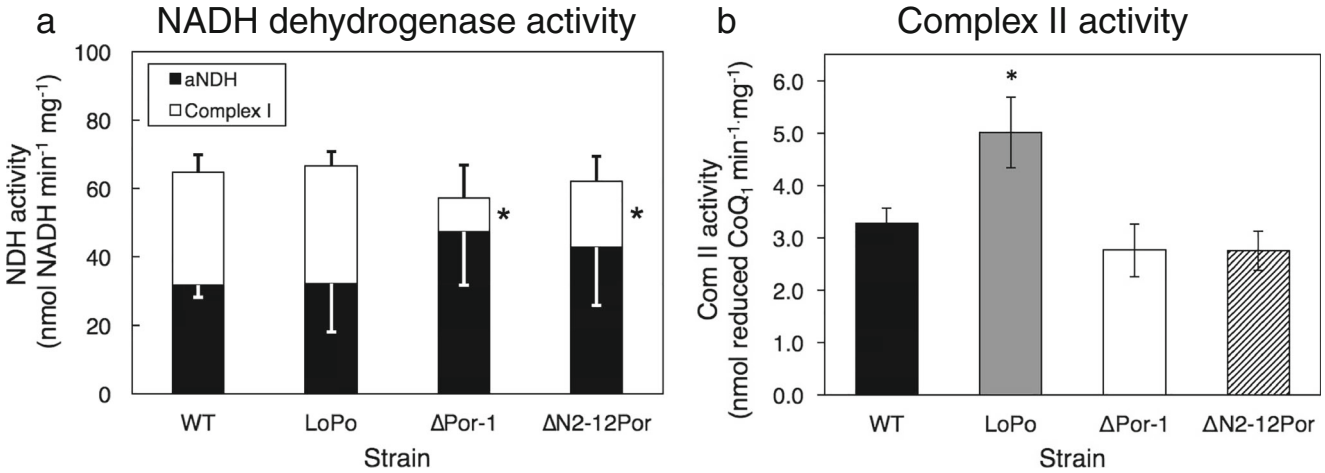

Fig. 4 Characterization of the ETC complexes of strains harbouring different variants of VDAC. **(a)** Complex I activity was determined as described in Materials and Methods and is presented as nmol of NADH oxidized per minute per mg of mitochondrial protein in the presence (black bars) and absence (sum of black and white bars) of rotenone. Rotenone-sensitive activity (white bars) was determined as the difference between the activities in the presence and absence of rotenone. Data represent the average activity measured from at least two biological replicates (independent mitochondrial isolations); in most cases two independent detergent extractions of each mitochondrial preparation were made, and each was analyzed in duplicate (technical replicates). The black and white error bars indicate the standard deviations for the rotenone insensitive, and sensitive activity, respectively. The error bars for each average are indicated only in one direction for clarity. The star indicates statistically different aNDH activity compared to WT. **(b)** Complex II activity was determined as described in Materials and Methods and is presented as nmole of CoQ_1 reduced per minute per mg of mitochondrial protein. Data represent averages and standard deviations of 3–4 biological replicates

combined activity of the four alternative NADH dehydrogenases in mitochondria (Fig. 1). Proteomic analysis (Ferens et al. 2017) revealed that the relative amounts of three of the four alternative NADH dehydrogenases (NDE1, NDE2, NDI1) were similar in ΔPor-1 and WT; the fourth enzyme, NDE3, was not detected in either strain. Therefore, to provide the additional rotenone-insensitive activity, the levels of NDE3 could be increased in ΔPor-1, or the activities of the detected proteins are increased, or a combination of the two events has occurred. In ΔPor-1, complex II activity was unchanged compared to WT (Fig. 4b). For clarity, results obtained from mitochondria from an additional variant, ΔN2-12Por, will be discussed separately at the end of the results section.

Substrates for determination of oxygen consumption and membrane potential

It was hypothesized that a reduction in, or the absence of, VDAC in the MOM would limit the first steps of substrate and ADP flow into mitochondria, and together with the associated defects in the ETC, would result in reduced membrane potential (Δψ) and/or an increased oxygen consumption rate (OCR). To investigate this, isolated mitochondria from WT, LoPo and ΔPor-1 were assessed in the presence of ETC substrates for complexes I and/or II (state 2 respiration), with substrate and ADP (state 3) and with substrate and oligomycin to pharmacologically induce a non-phosphorylating state of respiration (state 4o). In the first round of experiments (Supplementary Fig. 3), three substrate combinations were utilized to drive the ETC: i) succinate, which generates $FADH_2$ to be utilized by complex II, ii) glutamate and malate (GM), which generate NADH for complex I and iii) GMS, which activates both complexes I and II and is required for full operation of the TCA cycle (see (Chowdhury et al. 2016)). The data in Supplementary Fig. 3 represent mitochondria isolated from two independent cultures of *N. crassa* (biological replicates), and each biological replicate was examined in the presence of all three substrates. These observed trends, support the use of a combination of GMS as the substrate in the following experiments.

For mitochondria from all strains, the OCR (Supplementary Fig. 3a, state 2) was highest in GMS and in GM it was notably lower than in S alone or in GMS; this observation applied to all states of respiration. This pattern is expected, as glutamate-induced respiration generates NADH, which provides electrons for proton translocation (Joseph-Horne et al. 2001). In WT and LoPo mitochondria, the relative membrane polarization was similar in the presence of all substrates. Upon addition of ADP to initiate state 3 respiration, the membrane potential decreased (Supplementary Fig. 3b, state 3) and the OCR increased (Supplementary Fig. 3a, state 3), reflecting consumption of Δψ by ATP synthase (complex V), and electron flow to terminal oxygen. Inhibition of complex V by oligomycin (state 4o respiration) increased OCR and Δψ to levels similar observed in the substrate alone (Supplementary Fig. 3). In ΔPor-1 mitochondria, similar trends were observed, but the OCR was generally lower than that of WT utilizing S or GMS. Nonetheless, a response to ADP was observed in OCR and membrane polarization measurements, indicating that ADP was taken up and converted to ATP by these mitochondria.

Oxygen consumption and membrane potential

The OCR and Δψ for isolated LoPo and, unexpectedly ΔPor-1, mitochondria were similar to those of mitochondria isolated from the wild-type in GMS (Fig. 5, black bars). Upon addition of ADP to initiate state 3 respiration, the membrane potential decreased (Fig. 5a white bars) and the OCR increased (Fig. 5b white bars), relative to that in state 2, in all three types of mitochondria, reflecting consumption of Δψ by complex V/ATP synthase, and relaxation of respiratory control, thereby allowing electron flow to terminal oxygen. Although this indicates that ADP was able to cross the mitochondrial outer and inner membranes in the ΔPor-1 organelles, the increase in OCR and concomitant decrease in Δψ were less in ΔPor-1 mitochondria than those observed in the WT and LoPo organelles (Fig. 5), suggesting decreased depolarization due to impaired uptake of ADP or limitation of complex V flux. In all three mitochondrial types, inhibition of complex V by oligomycin (state 4o respiration) returned OCR and Δψ to levels observed in substrate alone (Fig. 5 grey bars). In mammalian cells, the respiratory control rate RCRo (OCR in state 3/OCR in state 4o) is used to assess coupling efficiency in mitochondria. When the RCRo was calculated using paired OCR data from the same preparation, a small, statistically significant difference was observed between ΔPor-1 (RCRo 1.71 ± 0.15) and WT (1.98 ± 0.08) mitochondria (Supplementary Table 1). However, this value is less useful for comparison in *N. crassa,* because, in contrast to WT, ΔPor-1 displays high levels of cyanide-resistant respiration, and thus oxygen consumption likely also occurs through AOX.

Mitochondrial ROS production

Links between VDAC and mitochondrial ROS production have been shown in yeast VDAC knockout strains, animal VDAC knockdown cell lines and yeast strains expressing different variants of VDAC (Galganska et al. 2008; Reina et al. 2010; Shoshan-Barmatz et al. 2010). Considering only the ETC defects, ΔPor-1 mitochondria are expected to lead to a highly reduced Q pool with a high ratio of CoQ(red)/CoQ(ox), leading to increased ROS production (see Fig. 2). However, the activity of AOX is predicted to ameliorate this effect, by oxidizing CoQ through transfer of electrons to molecular oxygen (see (Joseph-Horne et al. 2001)). To examine the net

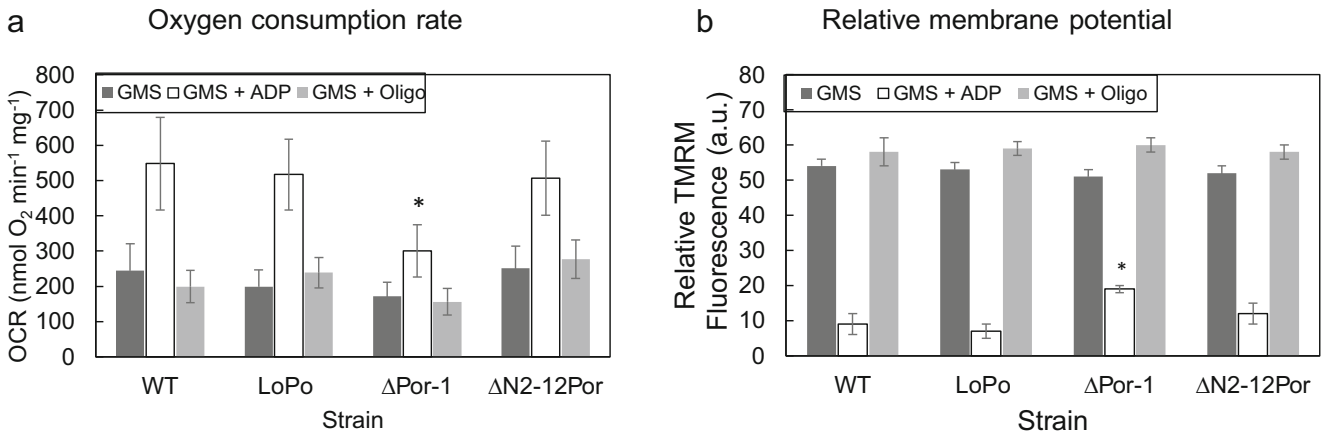

Fig. 5 Simultaneous measurements of membrane potential and oxygen consumption rates of mitochondria utilized in H_2O_2 generation experiments. **a** Oxygen consumption rates in mitochondria. OCR was measured as described in materials and methods, following sequential addition of substrate, ADP and oligomycin. The data presented are averages of 3 biological replicates for WT and LoPo and 4 biological replicates for ΔPor-1 and ΔN2-12Por, and the bars indicate the corresponding standard deviations. The star indicates a statistically significant difference between the relative OCR of the mutant and WT (students t-test, $p < 0.05$). **b** Mitochondrial ΔΨ as estimated by quenching of the fluorescent dye TMRM. For each of the indicated strains, the black bars indicate the relative TMRM fluorescence in the presence of GMS ($\Delta F_A/F_T \times 100$; see Fig. 3), the white bars show the degree of quenching of fluorescence (depolarization of mitochondria) in the presence of ADP ($\Delta F_B/F_T \times 100$), and the grey bars represent the quenching observed in the presence of oligomycin ($\Delta F_C/F_T \times 100$)

effects, the ROS released was measured from isolated mitochondria containing different levels of VDAC. Hydrogen peroxide efflux was measured after dismutation of superoxide to hydrogen peroxide, which we use the general term ROS to describe. Hydrogen peroxide levels are reasonable representatives of ROS production because superoxide is rapidly converted to H_2O_2 in mitochondria. However, one drawback of this approach is that only extramitochondrial H_2O_2 is measured (Munro and Treberg 2017) and VDAC is implicated in the release of ROS by mitochondria (Han et al. 2003), so the approach may under-represent ROS production by the variant mitochondria.

To probe the potential for ETC-derived ROS production, H_2O_2 production was measured in mitochondria respiring on GMS, with and without inhibitors that block electron flow. In complex I, there are two sites (I_F and I_Q) involved in ROS production; electrons flow from NADH to the flavin mononucleotide site (I_F) to the ubiquinone site (I_Q) to the Q-pool (Fig. 2, (Treberg et al. 2011)). In mammalian mitochondria, in the presence of the complex II substrate succinate, ROS is produced at the I_Q site due to reverse electron flow from the reduced Q-pool and the addition of rotenone decreases ROS production from that site by blocking the reverse flow (Liu et al. 2002; Lambert and Brand 2004). In contrast, rotenone increases ROS production in the presence of NADH-generating substrates, such as malate and glutamate, as it blocks the electron transfer from complex I to the Q-pool (Liu et al. 2002). Antimycin A was used to impair electron flow from complex III (Fig. 2). Antimycin A binds to the Q_i site of this complex, which may elevate superoxide formation from its Q_o site, and inhibits the mitochondrial electron transfer between cytochromes *b* and *c* (Quinlan et al. 2011; Ma et al. 2011). The rate of production of ROS from antimycin A-impaired complex III is increased in the presence of high membrane potential (reviewed in (Bleier and Drose 2013) and is impacted by the redox state of the Q-pool, reaching a maximum at intermediate levels of Q-pool reduction (Quinlan et al. 2011).

In wild-type *N. crassa* mitochondria, there was detectable H_2O_2 efflux, in the presence of GMS (Fig. 6, black bar). This rate decreased slightly in the presence of rotenone (white bar), suggesting that a proportion of ROS was generated by reverse flow of electrons from complex II to

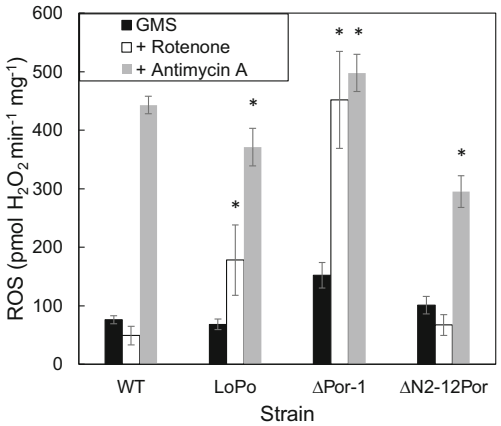

Fig. 6 ROS production by mitochondria isolated from WT and VDAC mutant strains. Mitochondria from the indicated strains were incubated in substrate alone (GMS; black bars), GMS and rotenone (white bars), or GMS and antimycin A (grey bars). ROS, represented by hydrogen peroxide, was measured as described in materials and methods. Values are averages of 3 (WT and LoPo) or 4 (ΔPor-1 and ΔN2-12Por) biological replicates; stars indicate values that differ from the corresponding WT value at a confidence level of $p < 0.05$ (Student's t test)

the Q-pool to complex I in the presence of GMS (see Fig. 2). Addition of antimycin A (grey bar) resulted in an almost 6-fold increase in ROS production over that in the presence of GMS alone, as expected in the absence of AOX. In LoPo mitochondria, the rate of ROS production, and the electron leak (Table 2) produced in the presence of GMS were similar to those of WT, but, in the presence of rotenone, ROS was generated at a rate about three times higher than for WT. This suggests that the I_Q site in complex I plays a larger role in ROS production in LoPo. This strain has high complex II activity (Fig. 4b), which may increase the proportion of electrons entering the Q-pool from this complex and thus, reverse flow into complex I may be increased, leading to an increase in the generation of ROS in the presence of rotenone. The addition of antimycin A to LoPo mitochondria in GMS caused an approximately 5-fold increase in ROS production compared to substrate alone, reflective of the wild-type levels of complex III and the absence of significant cyanide-insensitive, AOX activity in this strain (Table 1). The antimycin A-linked ROS production was somewhat lower than that from WT mitochondria; the reason for this is not known.

In contrast, ΔPor-1 mitochondria produced ROS at about twice the WT rate in the presence of GMS alone (Fig. 6), and the calculated electron leak was higher (Table 2). This is presumably due to reduced amounts of complexes III and IV, leading to a highly reduced Q pool with a redox state that is not maintained at wild-type levels. If this is the case, the AOX activity is insufficient to keep the ratio of CoQ(red)/CoQ(ox) as low as in WT. The ROS production rate tripled in the presence of rotenone, indicating that, when respiring on GMS, NADH-dependent sites of ROS are responsible for a significant portion of the reduction occurring from the Q-pool. If so, it is occurring in spite of increased aNDH activity and reduced levels of intact complex I (some subunits are at 1/16 to 1/32 of WT levels as estimated by mass spectroscopy; Ferens et al. 2017).

Table 2 Fractional electron leak in the presence of GMS

Strain	Electron leak relative to WT[a]
WT	100%
ΔPor-1	356 ± 130%[b] *
ΔN2-12porin	153 ± 20%[b] *
LoPo	100 ± 2%[b]

[a] relative electron leak was determined as the ratio between H_2O_2 produced and oxygen consumed, per mg mitochondria per minute; the value for WT mitochondria was $6.55*10^{-4}$ nmole H_2O_2 produced (nmole O consumed)$^{-1}$ and was set to 100%

[b] % of WT; stars indicate values that are different from WT, $p <= 0.05$

In ΔPor-1 mitochondria, the addition of antimycin A also induced an approximately 3.5-fold increase in ROS production compared to that of the GMS-treated mitochondria; this level is about 12% higher than that of WT. It was expected that ROS production would be controlled in part due to removal of electrons from the Q-pool by AOX activity. Further, ΔPor-1 mitochondria contain about 150% of WT levels of cytochrome *c* (Summers et al. 2012), which could scavenge some of the ROS produced by these defective ETC (see (Bleier and Drose 2013) for discussion).

Membrane potential, bioenergetics and ROS in ΔN2-12Por mitochondria

The expression of a truncated version of VDAC (ΔN2-12porin) partially restores growth of a ΔPor-1 strain (Shuvo et al. 2017). The N-terminus of VDAC resides in the lumen of the barrel, where it is hypothesized to control gating of the pore, and regulate interactions with ATP (reviewed by (Shuvo et al. 2016)). In artificial membranes, ΔN2-12porin produces gated, anion-selective pores with conductances of similar to size to those of the WT; however, individual channels are "noisy" with small, rapid fluctuations in current, suggesting a degree of channel instability (Popp et al. 1996). The ΔN2-12Por strain expresses relatively low (~10%) levels of ΔN2-12porin, has cytochrome aa_3 and *b* deficiencies and AOX expression similar to ΔPor-1 (Shuvo et al. 2017). Thus, the ΔN2-12porin strain was expected to provide an interesting intermediate between LoPo and ΔPor-1.

ΔN2-12porin mitochondria display a statistically significant decrease in complex I activity (Fig. 4a), although tNDH activity is similar to that of the other strains. Complex II activity is indistinguishable from WT. In GMS, (Fig. 5), significant differences were not observed in OCR and Δψ between WT and ΔN2-12porin; this trend was also seen for mitochondria in GM or S (Supplementary Fig. 3). Of particular interest are the data obtained under state 3 conditions, which indicate that the influence of ADP flow into mitochondria is similar to that in WT and more pronounced than in ΔPor-1, despite a much lower quantity of VDAC in the MOM of ΔN2-12Por. ROS production in GMS was somewhat higher than that of both WT and LoPo mitochondria, but was less than that of ΔPor-1 mitochondria (Fig. 6). The increased levels of ROS production seen in LoPo and ΔPor-1 mitochondria in the presence of rotenone were not observed in ΔN2-12Por mitochondria. While antimycin A induced a 3-fold increase in ROS in ΔN2-12Por, the rate was significantly lower than that observed in WT and ΔPor-1.

Discussion

Analysis of respiratory complexes I and II in VDAC variant mitochondria

Although complex I activity is reduced in ΔPor-1 cells (Fig. 4), the total activity of rotenone-insensitive aNDH is increased, presumably to maintain sufficient NADH/NAD^+ ratios. The 50% reduction in VDAC found in LoPo was unexpectedly found to be linked to an increase in complex II activity. However, the normal levels of complex II in ΔPor-1 cells suggest that there are threshold levels of VDAC at which different cellular responses, including increased AOX expression and altered complex II activity, occur. One intriguing explanation derives from the link between VDAC and complex II activity via the mTOR pathway. *Drosophila* cells in which the mTOR pathway is downregulated with rapamycin, display increased complex II activity, and reduced hydrogen peroxide production (Villa-Cuesta et al. 2014). In mammalian cells, the mTOR pathway is negatively regulated by itraconazole, which binds to VDAC1 (Head et al. 2015), suggesting that the status of VDAC is a player in mTOR regulation.

Membrane potential and OCR in VDAC variants

VDAC is a primary transport mechanism across the MOM for ADP, ATP and the small organic anions that include respiratory substrates. Considering this, and the slow growth rates of the ΔPor-1 strain (Summers et al. 2012), it was unexpected that ΔΨ and OCR in the non-phosphorylating state 2 and in the presence of oligomycin (state 4o) were similar in ΔPor-1 and WT mitochondria (Fig. 5; similar trends in seen in Supplementary Fig. 3). Furthermore, the activity of AOX (Summers et al. 2012; Ferens et al. 2017) and a reduced level of complex I (Ferens et al. 2017 and see Fig. 4a) would be expected to reduce proton translocation per oxygen consumed, and therefore would suggest a lower ΔΨ and/or a higher OCR. Neither of these was observed. In terms of OCR, in ΔPor-1, this rate is determined by the flux of electrons mediated by AOX and complex IV. The relative rates from each oxidase are not known, as respiration in the presence of cyanide (Table 1) does not reflect the distribution of electron flux between the two oxidases under inhibitor-free conditions, due to potential difference in the affinities for reduced quinones. In addition, the levels of active complex IV in ΔPor-1 cannot be predicted from the low levels of cytochromes aa_3 (~20%, Summers et al. 2012) in that strain. While data are not available for the *Neurospora* enzyme, the Km for reduced quinones may be at least 20-fold higher for AOX (~400 μM) than for complex III (<20 μM; discussed in (El-Khoury et al. 2013)). Thus, the proton-pumping complex III/complex IV arm of the ETC may predominate, ensuring sufficient membrane potential.

In mammalian cells, the respiratory control rate RCRo (OCR in state 3/OCR in state 4o) is used to assess coupling efficiency in mitochondria. When the RCRo was calculated using paired OCR data from the same preparation, a small, statistically significant difference was observed between ΔPor-1 (RCRo 1.71 ± 0.15) and WT (1.98 ± 0.08) mitochondria (Supplementary Table 1). However, this value is less useful for comparison in *N. crassa,* and perhaps other fungi and plants, because of cyanide-insensitive respiration, and oxygen consumption that occurs through AOX, without directly translocating protons.

The steady state membrane potential is a function of proton translocation into the IMS, and the sum of proton return through coupled processes such as ATP synthesis, protein import and transport of metabolites, as well as proton leak, through anion carriers for example (Joseph-Horne et al. 2001; Jastroch et al. 2010). In isolated mitochondria respiring in the absence of ADP, it would be expected that proton leak is a significant component of proton return to the matrix. In ΔPor-1 mitochondria, AOX is active, and therefore the ratio of protons translocated to electrons entering the ETC is lower. Therefore, assuming similar electron flux in the two strains, the maintenance of a potential similar to WT by ΔPor-1 mitochondria might indicate that the latter mitochondria are less prone to proton leak, perhaps through differences in lipid or protein composition of the inner membrane. However, it is important to consider that these experiments were performed with isolated mitochondria, and therefore describe the maximal OCR and Δψ under conditions in which substrates are not limiting and there is limited collapse of the proton motive force. Evidence obtained from cell lines may support the importance of this experimental difference; for example, the knockdown of VDAC isoform 1 from HepG2 and HeLa cell lines resulted in lower mitochondrial ΔΨ (Maldonado et al. 2013; Tewari et al. 2017). It is difficult to compare these data with those from the current study because phosphorylation state of the mitochondria and the effect of knockdown of VDAC on ETC complexes were not presented.

A second hypothesis was that the effect of externally-added ADP on ΔΨ would be reduced in the mitochondria lacking the normal amount of VDAC, because VDAC is considered to be a regulating step in the control of the flow of ATP across the MOM, and through the inner membrane (MIM) possibly via a complex between VDAC and the MIM protein, adenine nucleotide translocator (ANT) (Klingenberg 2008). As expected, the degree of depolarization observed in ΔPor-1 mitochondria was blunted compared to WT in the presence of ADP. Although it has long been understood that VDAC is a main pore in the MOM (discussed by (Krüger et al. 2017)), the fact that *Saccharomyces cerevisiae* lacking both isoforms of VDAC (Por1p and Por2p; (Blachly-Dyson et al. 1997), as

well as ΔPor-1 *N. crassa* (Summers et al. 2012), survive on non-fermentable carbon sources indicates that substrates and products of mitochondrial metabolism must enter and exit the organelle in its absence. This has been confirmed for NADH in Δ*por1* yeast mitochondria (Lee et al. 1998) and ADP via the induction of state 3 respiration in both fungi ((Michejda et al. 1990), this work).

Alternative mechanisms for the transit of adenine nucleotides and NADH across *Δpor1* yeast MOM have been based on the assumption that Por2p is not sufficient for these activities (Kmita et al. 1999) as its pore-forming activity was not confirmed (Blachly-Dyson et al. 1997). However, it was recently shown that Por2p (yVDAC2) forms pores that are generally similar to those of Por1p, and the lack of complementation of the *ΔPor1* mutant by Por2p may be related to the lack of expression of Por2p under normal conditions (Guardiani et al. 2018). In addition, conditions producing oxidized cytosolic environments in yeast increased levels of two other β-barrel proteins involved in mitochondrial protein import and assembly, Tom40 (translocase of the MOM) and Sam50/Tob55 (topogenesis of MOM beta-barrel proteins) were observed in *Δpor1* cells (Budzinska et al. 2007; Galganska et al. 2010), suggesting that the increased expression of these pores compensates for the lack of Por1p. However, similar increases in these proteins, and another MOM β-barrel, Mdm10, were not seen in proteomics assays of WT and ΔPor-1 mitochondria from *N. crassa* cells grown under the same conditions as those used in the analysis of ROS production (Summers et al. 2012; Ferens et al. 2017). Recently, non-β-barrel channels were identified in the MOM (Krüger et al. 2017) and it is possible that they are involved in transport across the MOM in the absence of VDAC. Two of these proteins, Ayr1 (*N. crassa* NCU07904) and Mim1 (NCU01101) are found at similar levels in WT and ΔPor-1 *N. crassa* cells (Shuvo et al. in preparation), indicating that they are not upregulated to compensate for the absence of VDAC in this fungus. Additional unidentified channels (Krüger et al. 2017) may be involved, or interactions between mitochondria and vacuoles or the endoplasmic reticulum, through contact structures (reviewed by (Elbaz-Alon 2017)) may provide flux of some mitochondrial substrates and products in vivo.

The ΔN2-12porin mitochondria were predicted to be an interesting intermediate between WT and ΔPor-1. However, mitochondrial depolarization upon addition of ADP was similar to WT, despite the presence of only 10% of WT levels of a truncated VDAC (Shuvo et al. 2017). Presumably, functional VDAC molecules, alone or in contact sites with ANT, are present in sufficient amounts in ΔN2-12porin (and LoPo) mitochondria to ensure that ATP/ADP exchange and respiratory substrate supply were not limiting factors for respiration.

Release of ROS by variant mitochondria

In the presence of GMS, the ROS production capacity for WT and LoPo were similar, as expected from the similar OCR and $\Delta\psi$ in the two strains (Fig. 6). LoPo expresses increased levels of complex II, which may have an impact on in electron flow, as suggested by the increase in ROS in the presence of rotenone, a complex I inhibitor, and by the small decrease in ROS induced by antimycin A (Fig. 6). Thus differences in the ETC complexes, or other NADH-dependent ROS production sites, exist that are not reflected in its essentially wild-type growth and respiratory phenotypes (Shuvo et al. 2017). In contrast, the severity of ETC defects in ΔPor-1 mitochondria is associated a higher fractional electron leak (Table 2) and ROS production (Fig. 6). It was striking that, although ΔPor-1 has relatively low amounts of complex I, H_2O_2 efflux is elevated 9-fold in the presence of rotenone. One possible explanation is that in the presence of rotenone, the NADH/NAD^+ ratio increased, leading to additional ROS production from other NADH-dependent ROS-producing sites, such as pyruvate dehydrogenase and α-ketoglutarate dehydrogenase (Brand 2010; Mailloux 2015). Another possibility is that activity of the aNDHs increases electron flow into the Q-pool, generating a higher ratio of CoQ(red)/CoQ(ox), which in turn could increase ROS production from complex II or III. Finally, it is also possible that partially assembled versions of complex I remain and have enhanced binding to rotenone; subunit composition has been associated with differential rotenone binding (Earley and Ragan 1984). Antimycin A treatment of ΔPor-1 mitochondria induced a rate of ROS production similar to that seen with rotenone; this was about 12% higher than that for WT in the presence of the complex III inhibitor. Thus, electrons from the coQ(red) are accessing complex III, even in the presence of AOX.

ΔPor-1 mitochondria have AOX activity, but assuming relatively low binding affinity for reduced CoQ (see above), the Q-pool may remain highly reduced. This could magnify the ROS production induced by antimycin A because reduced CoQ can interact with the higher affinity complex III, but the electrons are impaired from leaving it. This would lead to marked elevation in the production of ROS from Q_o site of complex III. Taken together, these data suggest that AOX can partially limit ROS production in uninhibited ΔPor-1 mitochondria, but cannot compensate for the highly reduced Q-pools expected when both pathways of Q oxidation, reverse flow through complex I and complex III activity, are blocked by the combination of inhibitor and mitochondrial defects (see Figs. 1 and 2).

The ΔN2-12porin mitochondria show an intermediate profile in terms of ROS production. There is a slight increase in ROS in GMS and in the presence of rotenone compared to WT. It is unclear whether the small increase can be linked to the small amount of VDAC or the N-terminal truncation, but it

is noteworthy that the increased ROS release is much less than that from ΔPor-1 mitochondria. Interestingly, the ROS production from antimycin-A treated mitochondria is less than that of WT, as expected if there is a lower level of complex III (based on cytochrome *b* levels). Further, AOX is expected to maintain electron flow in the upstream ETC complexes and thereby reduce ROS production relative to an equivalent system lacking AOX activity.

In spite of the differences between *S. cerevisiae* and *N. crassa* mitochondria, there are notable similarities in the bioenergetics of the wild-type and ΔPor1p or ΔPor-1 strains (collectively referred to as ΔPor for this discussion). In both organisms, the OCR is close to WT in the ΔPor strain (85–90% in *S. cerevisiae*) (Michejda et al. 1990), (Fig. 5a). This similarity is interesting, given the differences in electron transport in the two organisms. The activity of AOX in *N. crassa* would presumably reduce the number of protons pumped into the intermembrane space per oxygen molecule consumed in ΔPor-1, while yeast lack both complex I and AOX. Possible explanations for this observation include less proton leak and/or lower utilization of ΔΨ in ΔPor-1 *N. crassa* mitochondria. Further similarities extend to the changes in redox state associated with the lack of VDAC. In yeast, Por1p and Por2p mediate cytosolic and mitochondrial redox states in a manner that is growth-phase specific (Budzinska et al. 2007; Galganska et al. 2008). In *N. crassa*, there is a remarkably high increase in ROS production in ΔPor-1 mitochondria (Fig. 6), which may reflect complex I activity, which is not present in yeast.

Summary

The results presented herein form a detailed description of the impact of changes to the status of the most abundant MOM protein, VDAC, on mitochondrial bioenergetics and on ROS production by the mitochondria. In the absence of VDAC, increased activity of alternative NDH compensates for a decrease in complex I. Membrane potentials similar to those in WT are maintained in ΔPor-1 mitochondria, but consumption of the proton gradient is reduced in state 3 mitochondria, presumably due to reduced flow of substrates and products across the mitochondrial membranes. This correlates well with the reduced growth rates associated with the absence of porin. Furthermore, AOX activity is unable to completely reduce the excess ROS production associated with the defective ETC in ΔPor-1. A strain expressing VDAC at levels about 50% of WT shows increased complex II activity, and increased levels of ROS release when treated with rotenone. An N-terminal truncation variant displayed bioenergetics and ROS production capacity intermediate to those of WT and ΔPor-1, indicating that low levels of this protein, likely in conjunction with AOX activity, are able to maintain significant mitochondrial function in fungal cells.

Acknowledgements This work was supported by Discovery Grants (DG) from the Natural Sciences and Engineering Research Council of Canada (NSERC) to DAC and JRT, the Canada Research Chairs (CRC) program to JRT and the Faculty of Science (DC). SRS acknowledges support from the Faculty of Graduate Studies at the University of Manitoba and DG funds awarded to DAC. LMW was supported by DG and CRC funds to JRT. The authors thank Mr. Erwin J. Taguiam, Department of Microbiology, for excellent technical assistance, Dr. Frank Nargang, University of Alberta, for antibodies, and Dr. Richard Sparling, Department of Microbiology, for very valuable discussions and reading of the manuscript.

References

Banh S, Treberg JR (2013) The pH sensitivity of H_2O_2 metabolism in skeletal muscle mitochondria. FEBS Lett 587:1799–1804. https://doi.org/10.1016/j.febslet.2013.04.035

Banh S, Wiens L, Sotiri E, Treberg JR (2015) Mitochondrial reactive oxygen species production by fish muscle mitochondria: potential role in acute heat-induced oxidative stress. Comp Biochem Physiol B Biochem Mol Biol 191:99–107. https://doi.org/10.1016/j.cbpb.2015.10.001

Bayrhuber M, Meins T, Habeck M, Becker S, Giller K, Villinger S, Vonrhein C, Griesinger C, Zweckstetter M, Zeth K (2008) Structure of the human voltage-dependent anion channel. Proc Natl Acad Sci 105:15370–15375. https://doi.org/10.1073/pnas.0808115105

Blachly-Dyson E, Song J, Wolfgang WJ, Colombini M, Forte M (1997) Multicopy suppressors of phenotypes resulting from the absence of yeast VDAC encode a VDAC-like protein. Mol Cell Biol 17:5727–5738

Bleier L, Drose S (2013) Superoxide generation by complex III: from mechanistic rationales to functional consequences. Biochim Biophys Acta 1827:1320–1331. https://doi.org/10.1016/j.bbabio.2012.12.002

Brand MD (2010) The sites and topology of mitochondrial superoxide production. Exp Gerontol 45:466–472. https://doi.org/10.1016/j.exger.2010.01.003

Budzinska M, Galganska H, Wojtkowska M, Stobienia O, Kmita H (2007) Effects of VDAC isoforms on CuZn-superoxide dismutase activity in the intermembrane space of *Saccharomyces cerevisiae* mitochondria. Biochem Biophys Res Commun 357:1065–1070. https://doi.org/10.1016/j.bbrc.2007.04.090

Carneiro P, Duarte M, Videira A (2012) Disruption of alternative NAD(P)H dehydrogenases leads to decreased mitochondrial ROS in *Neurospora crassa*. Free Radic Biol Med 52:402–409. https://doi.org/10.1016/j.freeradbiomed.2011.10.492

Chowdhury SR, Djordjevic J, Albensi BC, Fernyhough P (2016) Simultaneous evaluation of substrate-dependent oxygen consumption rates and mitochondrial membrane potential by TMRM and safranin in cortical mitochondria. Biosci Rep 38:00286

Colombini M (1979) A candidate for the permeability pathway of the outer mitochondrial membrane. Nature 279:643–645

Colot HV, Park G, Turner GE, Ringelberg C, Crew CM, Litvinkova L, Weiss RL, Borkovich KA, Dunlap JC (2006) A high-throughput gene knockout procedure for *Neurospora* reveals functions for multiple transcription factors. Proc Natl Acad Sci U S A 103:10352–10357. https://doi.org/10.1073/pnas.0601456103

Court DA, Kleene R, Neupert W, Lill R (1996) Role of the N- and C-termini of porin in import into the outer membrane of *Neurospora* mitochondria. FEBS Lett 390:73–77. https://doi.org/10.1016/0014-5793(96)00629-1

Davis RH, de Serres FJ (1970) Genetic and microbiological research techniques for *Neurospora crassa*. Methods Enzymol 17:79–143. https://doi.org/10.1016/0076-6879(71)17168-6

Earley FG, Ragan CI (1984) Photoaffinity labelling of mitochondrial NADH dehydrogenase with arylazidoamorphigenin, an analogue of rotenone. Biochem J 224:525–534. https://doi.org/10.1042/bj2240525

Elbaz-Alon Y (2017) Mitochondria–organelle contact sites: the plot thickens. Biochem Soc Trans 45:477–488. https://doi.org/10.1042/BST20160130

El-Khoury R, Dufour E, Rak M et al (2013) Alternative oxidase expression in the mouse enables bypassing cytochrome c oxidase blockade and limits mitochondrial ROS overproduction. PLoS Genet 9: e1003182. https://doi.org/10.1371/journal.pgen.1003182

Ferens FG, Spicer V, Krokhin OV, Motnenko A, Summers WAT, Court DA (2017) A deletion variant partially complements a porin-less strain of *Neurospora crassa*. Biochem Cell Biol 95:318–327. https://doi.org/10.1139/bcb-2016-0166

Frazier AE, Thorburn DR (2012) Biochemical analyses of the electron transport chain complexes by spectrophotometry. Methods Mol Biol:49–62. https://doi.org/10.1007/978-1-61779-504-6_4

Galganska H, Budzinska M, Wojtkowska M, Kmita H (2008) Redox regulation of protein expression in *Saccharomyces cerevisiae* mitochondria: possible role of VDAC. Arch Biochem Biophys 479:39–45. https://doi.org/10.1016/j.abb.2008.08.010

Galganska H, Karachitos A, Wojtkowska M, Stobienia O, Budzinska M, Kmita H (2010) Communication between mitochondria and nucleus : putative role for VDAC in reduction / oxidation mechanism. BBA - Bioenerg 1797:1276–1280. https://doi.org/10.1016/j.bbabio.2010.02.004

Geula S, Ben-Hail D, Shoshan-Barmatz V (2012) Structure-based analysis of VDAC1: N-terminus location, translocation, channel gating and association with anti-apoptotic proteins. Biochem J 444:475–485. https://doi.org/10.1042/BJ20112079

Gonçalves AP, Videira A (2015) Mitochondrial type II NAD(P)H dehydrogenases in fungal cell death. Microb Cell 2:68–73. https://doi.org/10.15698/mic2015.03.192

Guardiani C, Magrì A, Karachitos A, di Rosa MC, Reina S, Bodrenko I, Messina A, Kmita H, Ceccarelli M, de Pinto V (2018) yVDAC2, the second mitochondrial porin isoform of *Saccharomyces cerevisiae*. Biochim Biophys Acta Bioenerg 1859:270–279. https://doi.org/10.1016/j.bbabio.2018.01.008

Han D, Antunes F, Canali R, Rettori D, Cadenas E (2003) Voltage-dependent anion channels control the release of the superoxide anion from mitochondria to cytosol. J Biol Chem 278:5557–5563

Harkness TAA, Nargang FE, Van Der Klei I et al (1994) A crucial role of the mitochondrial protein import receptor MOM19 for the biogenesis of mitochondria. J Cell Biol 124:637–648

Head SA, Shi W, Zhao L, Gorshkov K, Pasunooti K, Chen Y, Deng Z, Li RJ, Shim JS, Tan W, Hartung T, Zhang J, Zhao Y, Colombini M, Liu JO (2015) Antifungal drug itraconazole targets VDAC1 to modulate the AMPK/mTOR signaling axis in endothelial cells. Proc Natl Acad Sci 112:E7276–E7285. https://doi.org/10.1073/pnas.1512867112

Hiller S, Garces RG, Malia TJ, Orekhov VY, Colombini M, Wagner (2008) Solution structure of the integral human membrane protein VDAC-1 in detergent micelles. Science 321:1206–1210. https://doi.org/10.1126/science.1161302

Hoffman DL, Brookes PS (2009) Oxygen sensitivity of mitochondrial reactive oxygen species generation depends on metabolic conditions. J Biol Chem 284:16236–16245. https://doi.org/10.1074/jbc.M809512200

Jastroch M, Divakaruni AS, Mookerjee S, Treberg JR, Brand MD (2010) Mitochondrial proton and electron leaks. Essays Biochem 47:53–67. https://doi.org/10.1042/bse0470053

Joseph-Horne T, Hollomon DW, Wood PM (2001) Fungal respiration: a fusion of standard and alternative components. Biochim Biophys Acta 1504:179–195. https://doi.org/10.1016/S0005-2728(00)00251-6

Klingenberg M (2008) The ADP and ATP transport in mitochondria and its carrier. Biochim Biophys Acta Biomembr 1778:1978–2021. https://doi.org/10.1016/j.bbamem.2008.04.011

Kmita H, Stobienia O, Michejda J (1999) The access of metabolites into yeast mitochondria in the presence and absence of the voltage dependent anion selective channel (YVDAC1). Acta Biochim Pol 46: 991–1000 10824870

Krüger V, Becker T, Becker L, Montilla-Martinez M, Ellenrieder L, Vögtle FN, Meyer HE, Ryan MT, Wiedemann N, Warscheid B, Pfanner N, Wagner R, Meisinger C (2017) Identification of new channels by systematic analysis of the mitochondrial outer membrane. J Cell Biol 216:3485–3495. https://doi.org/10.1083/jcb.201706043

Lambert AJ, Brand MD (2004) Superoxide production by NADH:ubiquinone oxidoreductase (complex I) depends on the pH gradient across the mitochondrial inner membrane. Biochem J 382:511–517

Lee AC, Xu X, Blachly-Dyson E, Forte M, Colombini M (1998) The role of yeast VDAC genes on the permeability of the mitochondrial outer membrane. J Membr Biol 161:173–181. https://doi.org/10.1007/s002329900324

Liu Y, Fiskum G, Schubert D (2002) Generation of reactive oxygen species by the mitochondrial electron transport chain. J Neurochem 80:780–787. https://doi.org/10.1046/j.0022-3042.2002.00744.x

Ma X, Jin M, Cai Y, Xia H, Long K, Liu J, Yu Q, Yuan J (2011) Mitochondrial electron transport chain complex III is required for antimycin a to inhibit autophagy. Chem Biol 18:1474–1481. https://doi.org/10.1016/j.chembiol.2011.08.009

Mailloux RJ (2015) Teaching the fundamentals of electron transfer reactions in mitochondria and the production and detection of reactive oxygen species. Redox Biol 4:381–398. https://doi.org/10.1016/j.redox.2015.02.001

Maldonado EN, Sheldon KL, DeHart DN et al (2013) Voltage-dependent anion channels modulate mitochondrial metabolism in cancer cells: regulation by free tubulin and erastin. J Biol Chem 288:11920–11929. https://doi.org/10.1074/jbc.M112.433847

Marques I, Duarte M, Assunção J, Ushakova AV, Videira A (2005) Composition of complex I from Neurospora crassa and disruption of two "accessory" subunits. Biochim Biophys Acta Bioenerg 1707: 211–220. https://doi.org/10.1016/j.bbabio.2004.12.003

Marques I, Dencher NA, Videira A, Krause F (2007) Supramolecular organization of the respiratory chain in Neurospora crassa mitochondria. Eukaryot Cell 6:2391–2405

Maxwell DP, Wang Y, Mcintosh L, Kende HJ (1999) The alternative oxidase lowers mitochondrial reactive oxygen production in plant cells. Plant Biol 96:8271–8276

McCluskey K, Wiest A, Plamann M (2010) The fungal genetics stock center: a repository for 50 years of fungal genetics research. J Biosci 35:119–126

Michejda J, Guo XJ, Lauquin GJM (1990) The respiration of cells and mitochondria of porin deficient yeast mutants is coupled. Biochem Biophys Res Commun 171:354–361. https://doi.org/10.1016/0006-291X(90)91401-D

Møller IM (2001) Plant mitochondria and oxidative stress: Electron transport, NADPH turnover, and metabolism of reactive oxygen species. Annu Rev Plant Physiol Plant Mol Biol 52:561–591

Muller FL, Liu Y, Abdul-Ghani MA, Lustgarten MS, Bhattacharya A, Jang YC, Van Remmen H (2008) High rates of superoxide production in skeletal-muscle mitochondria respiring on both complex I- and complex II-linked substrates. Biochem J 409:491–499. https://doi.org/10.1042/BJ20071162

Munro D, Treberg JR (2017) A radical shift in perspective: mitochondria as regulators of reactive oxygen species. J Exp Biol 220:1170–1180. https://doi.org/10.1242/jeb.132142

Nargang FE, Rapaport D (2007) *Neurospora crassa* as a model organism for mitochondrial biogenesis. Methods Mol Biol 372:107–123

Popp B, Court DA, Benz R, Neupert W, Lill R (1996) The role of the N and C termini of recombinant *Neurospora* mitochondrial porin in channel formation and voltage-dependent gating. J Biol Chem 271: 13593–13599. https://doi.org/10.1074/jbc.271.23.13593

Quinlan CL, Gerencser AA, Treberg JR, Brand MD (2011) The mechanism of superoxide production by the antimycin-inhibited mitochondrial Q-cycle. J Biol Chem 286:31361–31372. https://doi.org/10.1074/jbc.M111.267898

Quinlan CL, Orr AL, Perevoshchikova IV, Treberg JR, Ackrell BA, Brand MD (2012) Mitochondrial complex II can generate reactive oxygen species at high rates in both the forward and reverse reactions. J Biol Chem 287:27255–27264. https://doi.org/10.1074/jbc.M112.374629

Reina S, Palermo V, Guarnera A, Guarino F, Messina A, Mazzoni C, de Pinto V (2010) Swapping of the N-terminus of VDAC1 with VDAC3 restores full activity of the channel and confers anti-aging features to the cell. FEBS Lett 584:2837–2844. https://doi.org/10.1016/j.febslet.2010.04.066

Schein SJ, Colombini M, Finkelstein A (1976) Reconstitution in planar lipid bilayers of a voltage-dependent anion-selective channel obtained from paramecium mitochondria. J Membr Biol 30:99–120. https://doi.org/10.1007/BF01869662

Schlossmann J, Dietmeier K, Pfanner N, Neupert W (1994) Specific recognition of mitochondrial preproteins by the cytosolic domain of the import receptor MOM72. J Biol Chem 269:11893–11901

Schneider H, Arretz M, Wachter E, Neupert W (1990) Matrix processing peptidase of mitochondria. Structure-function relationships. J Biol Chem 265:9881–9887

Shoshan-Barmatz V, De S (2017) Mitochondrial VDAC, the Na+/Ca2+ exchanger, and the Ca2+uniporter in Ca2+dynamics and signaling. Adv Exp Med Biol 981:323–347. https://doi.org/10.1007/978-3-319-55858-5_13

Shoshan-Barmatz V, De Pinto V, Zweckstetter M et al (2010) VDAC, a multi-functional mitochondrial protein regulating cell life and death. Mol Asp Med 31:227–285. https://doi.org/10.1016/j.mam.2010.03.002

Shuvo SR, Ferens FG, Court DA (2016) The N-terminus of VDAC: structure, mutational analysis, and a potential role in regulating barrel shape. Biochim Biophys Acta Biomembr 1858:1350–1361

Shuvo SR, Kovaltchouk U, Zubaer A, Kumar A, Summers WAT, Donald LJ, Hausner G, Court DA (2017) Functional characterization of an N-terminally truncated mitochondrial porin expressed in *Neurospora crassa*. Can J Microbiol 63:730–738. https://doi.org/10.1139/cjm-2016-0764

Summers WAT, Wilkins JA, Dwivedi RC, Ezzati P, Court DA (2012) Mitochondrial dysfunction resulting from the absence of mitochondrial porin in *Neurospora crassa*. Mitochondrion 12:220–229. https://doi.org/10.1016/j.mito.2011.09.002

Tanton LL, Nargang CE, Kessler KE, Li Q, Nargang FE (2003) Alternative oxidase expression in *Neurospora crassa*. Fungal Genet Biol 39:176–190. https://doi.org/10.1016/S1087-1845(03)00002-1

Tewari D, Majumdar D, Vallabhaneni S, Bera AK (2017) Aspirin induces cell death by directly modulating mitochondrial voltage-dependent anion channel (VDAC). Sci Rep 7:45184. https://doi.org/10.1038/srep45184

Tomasello MF, Guarino F, Reina S, Messina A, De Pinto V (2013) The voltage-dependent anion selective channel 1 (VDAC1) topography in the mitochondrial outer membrane as detected in intact cell. PLoS One 8(12):e81522. https://doi.org/10.1371/journal.pone.0081522

Treberg JR, Quinlan CL, Brand MD (2011) Evidence for two sites of superoxide production by mitochondrial NADH-ubiquinone oxidoreductase (complex I). J Biol Chem 286:27103–27110. https://doi.org/10.1074/jbc.M111.252502

Ujwal R, Cascio D, Colletier JP, Faham S, Zhang J, Toro L, Ping P, Abramson J (2008) The crystal structure of mouse VDAC1 at 2.3 A resolution reveals mechanistic insights into metabolite gating. Proc Natl Acad Sci 105:17742–7. https://doi.org/10.1073/pnas.0809634105

Videira A, Duarte M (2002) From NADH to ubiquinone in *Neurospora* mitochondria. Biochim Biophys Acta Bioenerg 1555:187–191. https://doi.org/10.1016/S0005-2728(02)00276-1

Villa-Cuesta E, Holmbeck MA, Rand DM (2014) Rapamycin increases mitochondrial efficiency by mtDNA-dependent reprogramming of mitochondrial metabolism in Drosophila. J Cell Sci 127:2282–2290. https://doi.org/10.1242/jcs.142026

Young MJ, Bay DC, Hausner G, Court DA (2007) The evolutionary history of mitochondrial porins. BMC Evol Biol 7:31